

## CHAPTER 200

### SEDIMENT TRANSPORT BY CURRENTS AND WAVES

Leo C. van Rijn<sup>1)</sup> and Aart Kroon<sup>2)</sup>

#### Abstract

Mathematical and experimental modelling of sediment transport processes in the coastal environment is presented. The convection-diffusion equation for suspended sediment particles has been used to compute the vertical distribution of the time-averaged concentrations. The computed results are compared with measured values of laboratory and field experiments (surf zone Dutch coast).

#### 1. Introduction

Many details of the complicated sediment transport processes in the coastal environment are still unknown. To get a better understanding of the most relevant processes, an integrated research programme has been set up, sponsored by the Coastal Genesis project (Rijkswaterstaat, The Netherlands), the MAST project (EEC research programme) and the Basic Research programme of Delft Hydraulics.

The research programme is focused on theoretical and experimental modelling of the processes involved. The major part of the work is related to experimental work, as follows:

- wave tunnel experiments to study the near-bed phenomena (Ribberink and Al Salem, 1991 and 1992)
- wave-current flume and basin experiments to study the vertical structure of the velocity and sediment concentration (Van Rijn et al, 1993)
- surf zone experiment near the Dutch coast (Kroon and Van Rijn, 1992).

Herein, the mathematical modelling of time-averaged sediment concentrations in the coastal environment is presented. The computed values are compared with measured results from laboratory and field experiments.

- 
- 1) Senior engineer, Delft Hydraulics, P.O. Box 152, 8300 AD Emmeloord, The Netherlands
  - 2) Researcher, Dep. Phys. Geography, Univ. of Utrecht, P.O. Box 80115, Utrecht, The Netherlands

## 2. Mathematical model

### 2.1 Transport processes

The total sediment transport rate ( $q_t$ ) can be computed from the vertical distribution of fluid velocities and sediment concentrations, as follows:

$$q_t = \int_0^{h+\eta} VC \, dz \quad (1)$$

in which:

- V = local instantaneous fluid velocity at height z above bed (m/s)
- C = local instantaneous sediment concentrations at height z above bed (kg/m<sup>3</sup>)
- h = water depth (to mean surface level) (m)
- $\eta$  = water surface elevation (m)

Defining:  $V = v + \tilde{v}$  and  $C = c + \tilde{c}$  (2)

in which:

- v = time and space-averaged fluid velocity at height z (m/s)
- c = time and space-averaged concentration at height z (m/s)
- $\tilde{v}$  = oscillating fluid component (including turbulent component) (m/s)
- $\tilde{c}$  = oscillating concentration component (including turbulent component) (m/s)

Substituting Eq. (2) in Eq. (1) and averaging over time and space, yields:

$$\bar{q}_t = \int_0^h \bar{v}c \, dz + \int_0^h \bar{\tilde{v}\tilde{c}} \, dz = \bar{q}_c + \bar{q}_w \quad (3)$$

in which:

$$\bar{q}_c = \int_0^h \bar{v}c \, dz = \text{time-averaged current-related sediment transport rate (kg/sm)}$$

$$\bar{q}_w = \int_0^h \bar{\tilde{v}\tilde{c}} \, dz = \text{time-averaged wave-related sediment transport rate (kg/sm)}$$

The current-related sediment transport is defined as the transport of sediment particles by the time-averaged (mean) current velocities (longshore currents, rip currents, undertow currents). The current velocities and the sediment concentrations are affected by the wave motion. It is known that the wave motion reduces the current velocities near the bed, but the wave motion strongly increases the near-bed concentrations due to its stirring action. The wave-related sediment transport is defined as the transport of sediment particles by the oscillating fluid components (cross-shore orbital motion).

In this paper the attention is focused on the current-related transport rate.

## 2.2 Time-averaged concentration profile

Usually, the convection-diffusion equation is applied to compute the equilibrium concentration profile in steady flow. This equation reads as:

$$w_{s,m} + \epsilon_{s,cw} \frac{dc}{dz} = 0 \quad (4)$$

in which:

$w_{s,m}$  = fall velocity of suspended sediment in a fluid-sediment mixture (m/s)

$\epsilon_{s,cw}$  = sediment mixing coefficient for combined current and waves (m<sup>2</sup>/s)

$c$  = time-averaged concentration at height  $z$  above the bed (kg/m<sup>3</sup>)

Here, it is assumed that Eq. (4) is also valid for wave-related mixing.

## 2.3 Sediment mixing coefficient

For combined current and wave conditions the sediment mixing coefficient is modeled as:

$$\epsilon_{s,cw} = [(\epsilon_{s,w})^2 + (\epsilon_{s,c})^2]^{0.5} \quad (5)$$

in which:

$\epsilon_{s,w}$  = wave-related mixing coefficient (m<sup>2</sup>/s)

$\epsilon_{s,c}$  = current-related mixing coefficient (m<sup>2</sup>/s)

First, the wave-related mixing is discussed.

Measurements in wave flumes show the presence of suspended sediment particles from the bed up to the water surface (Van Rijn, 1991). The largest concentrations are found close to the bed where the diffusivity is large due to ripple-generated eddies. Further away from the bed the sediment concentrations decrease rapidly because the eddies dissolve rather rapidly travelling upwards.

Various researchers have tried to model the suspension process by introducing an effective wave-related sediment mixing coefficient (see Van Rijn 1989 and 1993).

As the existing relationships do not yield acceptable results, a new approach was presented. Based on analysis of measured concentration profiles, the following characteristics were observed (Van Rijn, 1989, 1993);

- approximately constant mixing coefficient  $\epsilon_{s,w,bed}$  in a layer ( $z \leq \delta_s$ ) near the bed,
- approximately constant mixing coefficient  $\epsilon_{s,w,max}$  in the upper half ( $z \geq 0.5 h$ ) of the water depth,
- approximately linear variation of the mixing coefficient for  $\delta_s < z < 0.5 h$ .

The mathematical formulation reads as (see Figure 1):

$$z \leq \delta_s \quad \epsilon_{s,w} = \epsilon_{s,w,bed} \quad (6a)$$

$$z \geq 0.5 h \quad \epsilon_{s,w} = \epsilon_{s,w,max} \quad (6b)$$

$$\delta_s < z < 0.5 h \quad \epsilon_{s,w} = \epsilon_{s,w,bed} + [\epsilon_{s,w,max} - \epsilon_{s,w,bed}] \left[ \frac{z - \delta_s}{0.5h - \delta_s} \right] \quad (6c)$$

Equation (6) is fully defined when the following three parameters are known:

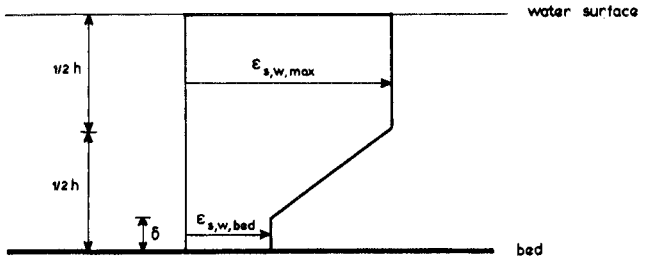
1. Thickness of near-bed sediment mixing layer ( $\delta_s$ ).  
Based on analysis of concentration profiles measured in non-breaking waves, it was found that:

$$\delta_s = 3 \Delta_r \quad (\text{ripple height})$$

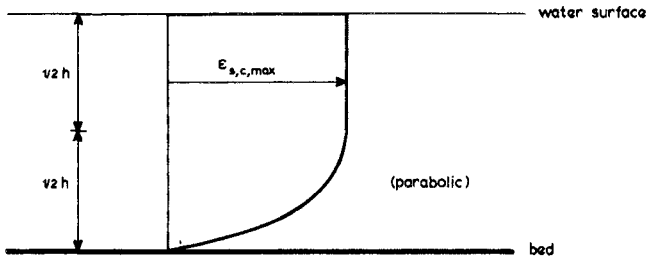
$$\delta_s = 3 \delta_w \quad (\text{sheet flow regime})$$

in which:

- $\Delta_r$  = ripple height (m)
- $\delta_w = 0.072 \hat{\Lambda}_s (\hat{\Lambda}_s / k_{s,w})^{-0.25}$  = wave boundary layer thickness (m)
- $\delta_s$  = thickness of near-bed sediment mixing layer (m)
- $k_{s,w}$  = wave-related bed roughness height (=  $3\Delta_r$  in ripple regime and  $\frac{1}{2} \delta_w$  in sheet flow regime) (m)



A. WAVE-RELATED SEDIMENT MIXING COEFFICIENT



B. CURRENT-RELATED SEDIMENT MIXING COEFFICIENT

Figure 1 Mixing coefficient distribution

2. Mixing coefficient in near-bed layer ( $\epsilon_{s,w,bed}$ )  
 This parameter was found to be:

$$\epsilon_{s,w,bed} = \alpha_b \hat{U}_\delta \delta_s \quad (8)$$

in which:

$\hat{U}_\delta$  = peak value of near-bed orbital velocity (based on significant wave height) (m/s)

$\alpha_b$  = 0.004  $D_*$  = empirical coefficient (-)

$D_*$  =  $d_{50} [(\rho_s - \rho)g / (\rho v^2)]^{1/3}$  = particle size parameter (m)

3. Mixing coefficient in upper layer ( $\epsilon_{s,w,max}$ )  
 This parameter was found to be:

$$\epsilon_{s,w,max} = 0.035 \frac{H_s h}{T_p} \quad (9)$$

in which:

$H_s$  = significant wave height (m)

$T_p$  = peak period of spectrum (s)

$h$  = water depth (m)

Second, the current-related mixing coefficient ( $\epsilon_{s,c}$ ) is presented, which reads as:

$$\epsilon_{s,c} = \kappa \beta u_{*,c} z(1-z/h) \quad \text{for } z < 0.5 h \quad (10)$$

$$\epsilon_{s,c} = 0.25 \beta \kappa u_{*,c} h \quad \text{for } z \geq 0.5 h$$

in which:

$u_{*,c}$  =  $(g^{0.5} \bar{v}_R) / C$  = bed-shear velocity (m/s)

$C$  =  $18 \log(12h/k_{s,c})$  = Chézy coefficient ( $m^{0.5}/s$ )

$\bar{v}_R$  = depth-averaged velocity (m/s)

$k_{s,c}$  = current-related bed-roughness height (m)

$h$  = water depth (m)

$\kappa$  = constant of Von Karman (= 0.4)

$\beta$  = coefficient ( $\approx 1$ )

#### 2.4 Reference concentration near the bed

The reference concentration is given by:

$$c_a = 0.015 \frac{d_{50}}{a} \frac{T^{1.5}}{D_*^{0.3}} \quad (11)$$

in which:

$D_*$  = dimensionless particle parameter (-)

$T$  = dimensionless bed-shear stress parameter (-)

$a$  = reference level (m)

The T-parameter is, as follows:

$$T = [\tau'_{b,cw} - \tau'_{b,cr}] / \tau_{b,cr} \quad (12)$$

in which:

$\tau'_{b,cw}$  = time-averaged effective bed-shear stress (N/m<sup>2</sup>)

$\tau'_{b,cr}$  = time-averaged critical bed-shear stress according to Shields (N/m<sup>2</sup>)

The magnitude of the time-averaged bed-shear stress, which is independent of the angle between the wave- and current direction is given by (Van Rijn, 1990):

$$\tau'_{b,cw} = \tau'_{b,c} + \tau'_{b,w} \quad (13)$$

in which:

$\tau'_{b,c} = \mu_c \alpha_{cw} \tau_{b,c}$  = effective current-related bed-shear stress (N/m<sup>2</sup>)

$\tau'_{b,w} = \mu_w \tau_{b,w}$  = effective wave-related bed-shear stress (N/m<sup>2</sup>)

$\tau_{b,c} = \frac{1}{8} \rho f_c (\bar{v}_R)^2$  = current-related bed-shear stress (N/m<sup>2</sup>)

$\tau_{b,w} = \frac{1}{4} \rho f_w (\hat{U}_\delta)^2$  = wave-related bed-shear stress (N/m<sup>2</sup>)

$f_c = 0.24 [\log(12h/k_{s,c})]^{-2}$  = current-related friction factor (-)

$f'_c = 0.24 [\log(12h/3d_{90})]^{-2}$  = grain friction factor (-)

$f_w = \exp[-6+5.2(\hat{\Lambda}_\delta/k_{s,w})^{-0.19}]$  = wave-related friction factor (-)

$\bar{v}_R$  = depth-averaged current-velocity (m/s)

$\hat{U}_\delta$  = peak value of near-bed orbital velocity (m/s)

$\hat{\Lambda}_\delta$  = peak value of near-bed orbital excursion (m)

$h$  = water depth (m)

$k_{s,c}$  = current-related bed-roughness (m)

$k_{s,w}$  = wave-related bed-roughness (m)

$\mu_c = f'_c/f_c$  = current-related efficiency factor (-)

$\mu_w = 0.6/D_*$  = wave-related efficiency factor (-)

$\alpha_{cw}$  = correction factor related wave-current interaction (see next section), (-)

$\rho$  = fluid density (kg/m<sup>3</sup>)

$\rho_s$  = sediment density (kg/m<sup>3</sup>)

## 2.5 Current velocity profile

The current velocity profile (see Fig. 2) is represented as a two-layer system to account for the wave effects in the near-bed layer (Van Rijn, 1993):

$$v(z) = \frac{\bar{v}_x \ln(30z/k_a)}{-1 + \ln(30h/k_a)} \quad \text{for } z \geq 3 \delta_w \quad (14)$$

$$v(z) = \frac{\bar{v}_x \ln(90\delta_w/k_a) \ln(30z/k_{s,c})}{[\ln(90\delta_w/k_{s,c})] [-1 + \ln(30h/k_a)]} \quad \text{for } z < 3 \delta_w$$

in which:

- $k_a = k_{s,c} \exp[\gamma \hat{U}_\delta / \bar{v}_r]$  = apparent roughness related to wave-current interaction ( $k_{a,max} = 10 k_{s,c}$ ) (m)
- $k_{s,c}$  = physical current-related bed roughness (m)
- $\gamma = 0.8 + \phi - 0.3 \phi^2$
- $\phi$  = angle between current and wave direction (in radians between 0 and  $\pi$ ;  $90^\circ = \frac{1}{2}\pi$ ,  $180^\circ = \pi$ )
- $\delta_w = 0.072 \hat{A}_\delta (\hat{A}_\delta / k_{s,w})^{-0.25}$  = maximum thickness of wave boundary layer (m)

The  $\alpha_{cw}$ -factor is given by (Van Rijn, 1993):

$$\alpha_{cw} = \left[ \frac{\ln(90 \delta_w / k_a)}{\ln(90 \delta_w / k_{s,c})} \right]^2 \left[ \frac{-1 + \ln(30h / k_{s,c})}{-1 + \ln(30h / k_a)} \right]^2 \tag{15}$$

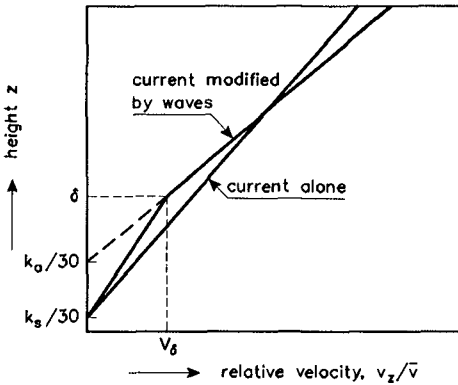


Figure 2 Velocity profile

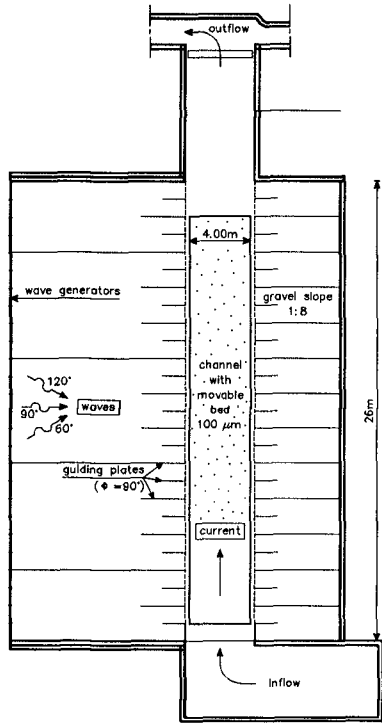


Figure 3 Plan view of wave-current basin

## 2.6 Sediment transport

The suspended load transport is given by:

$$q_{s,c} = \int_a^h vc \, dz \quad (16)$$

The bed-load transport is given by:

$$q_{b,c} = 0.25u'_{*,c} d_{50} T^{1.5} D_*^{-0.3} \quad (17)$$

in which:  $u'_{*,c} = (\tau'_{b,c}/\rho)^{0.5}$

## 3. Laboratory experiments

### 3.1 Experiments

Experiments were carried out in a wave-current basin at Delft Hydraulics to measure the current velocities and sediment concentrations under irregular non-breaking waves combined with a current. The bed material consisted of fine sand with  $d_{10} = 70 \mu\text{m}$ ,  $d_{50} = 100 \mu\text{m}$  and  $d_{90} = 130 \mu\text{m}$ . The water depth was about 0.4 m. Figure 3 shows a plan view of the experimental facility. The current was confined (by guiding plates) in a channel (width = 4 m) with a movable bed consisting of fine sand ( $d_{50} = 100 \mu\text{m}$ ). The guiding plates were placed normal to the wave crests. The (significant) wave heights generated were  $H_s = 0.07$ , 0.1 and 0.14 m. The peak period of the wave spectrum was about 2.3 s. Three current velocities (0.1, 0.2 and 0.3 m/s) were generated by varying the pump discharge. The velocity distribution across the channel was almost uniform. The velocity profiles in the middle of the channel were perfectly logarithmic. The vertical distribution of the turbulence intensity was in good agreement with values reported in the literature. Based on this, it was concluded that the effect of the guiding plates on the current was negligible. The wave propagation direction was set at  $60^\circ$ ,  $90^\circ$  and  $120^\circ$ .

The water entering the channel had no initial sediment load. Consequently, the concentration profiles were generated by erosion of sediment particles from the bed. To provide enough length for establishing equilibrium concentration profiles, the measuring section was situated at a distance of about 30 times the water depth from the channel entrance.

### 3.2 Instruments

Measurements of wave height, velocity and sediment concentration were performed from a carriage moving over rails above the channel. Water level variations were measured by use of a resistance probe near the location where the concentrations and velocities were measured (measuring period = 30 min). Characteristic wave parameters were computed from the data records.

Instantaneous sediment concentrations were measured by use of an acoustic probe; time-averaged sediment concentrations were determined from water-sediment samples using a pump sampler. This latter instrument consisted of an array of ten intake tubes of 3 mm internal diameter connected to the pumps by plastic hoses. The lowest intake tube was placed at about 0.01 m above the crest level of the bed forms. The intake openings were placed in transverse direction to the plane of orbital motion (Bosman et al, 1987). The intake velocity was about 1 m/s satisfying sampling requirements. The 10 liter samples were collected in calibrated buckets.

Instantaneous velocities were measured using an electromagnetic velocity meter (EMS) with a measuring level of about 3 mm below the probe and an acoustical probe (AZTM). The velocities were measured at the same elevations above the mean bed as those of the concentrations starting at the lowest point and working upwards. A time-averaging period of 256 s (approx. 100 waves) was applied.

Space averaging over the bed-form length was performed by moving the sediment concentration and fluid velocity instruments forward and backward over a certain longitudinal distance by use of an oscillating carriage above the channel. The velocity of the moving carriage (approx. 0.01 m/s) was small compared with the fluid velocity and large compared with the bed-form migration velocity. The error in the time-averaged velocity was less than 0.00125 m/s in the present tests. Preliminary tests showed that a space-averaging distance of 0.6 m (approx. 5 ripple lengths) was sufficiently large to give reproducible results.

### 3.3 Time-averaged concentration profiles

Analysis of the time-averaged concentration profiles shows the following results:

- concentrations increase for increasing wave height,
- current velocity does not affect the near-bed concentration; increasing current velocity results in a more uniform concentration profile (larger mixing),
- concentrations are largest when the wave direction is normal to the current direction.

Measured concentration profiles for four tests are shown in Fig. 4. Equation (4) was used to compute the time-averaged concentration profiles based on the following input data:  $d_{50} = 100 \mu\text{m}$ ,  $d_{90} = 130 \mu\text{m}$ ,  $w_s = 0.0065 \text{ m/s}$ ,  $k_{s,w} = k_{s,c} = 3\Delta_r$ ,  $\Delta_r$  = measured ripple height,  $a = 0.5\Delta_r$ ,  $\delta_s = 3\Delta_r$ ,  $\rho = 1000 \text{ kg/m}^3$ ,  $\rho_s = 2650 \text{ kg/m}^3$ .

The Bijker method (1971, 1978) was also used to compute the concentration profiles. The b-coefficient of this method was used as a calibration coefficient. A value of  $b = 1$  gave the best results.

The computed concentration profiles are shown in Fig. 4. Both methods yield reasonable results; the method of Bijker overestimates the measured concentrations at low velocities of 0.1 m/s (T14 10 90).

Computed transport rates showed reasonable agreement with measured values; most computed values are within a factor 2 of measured values.

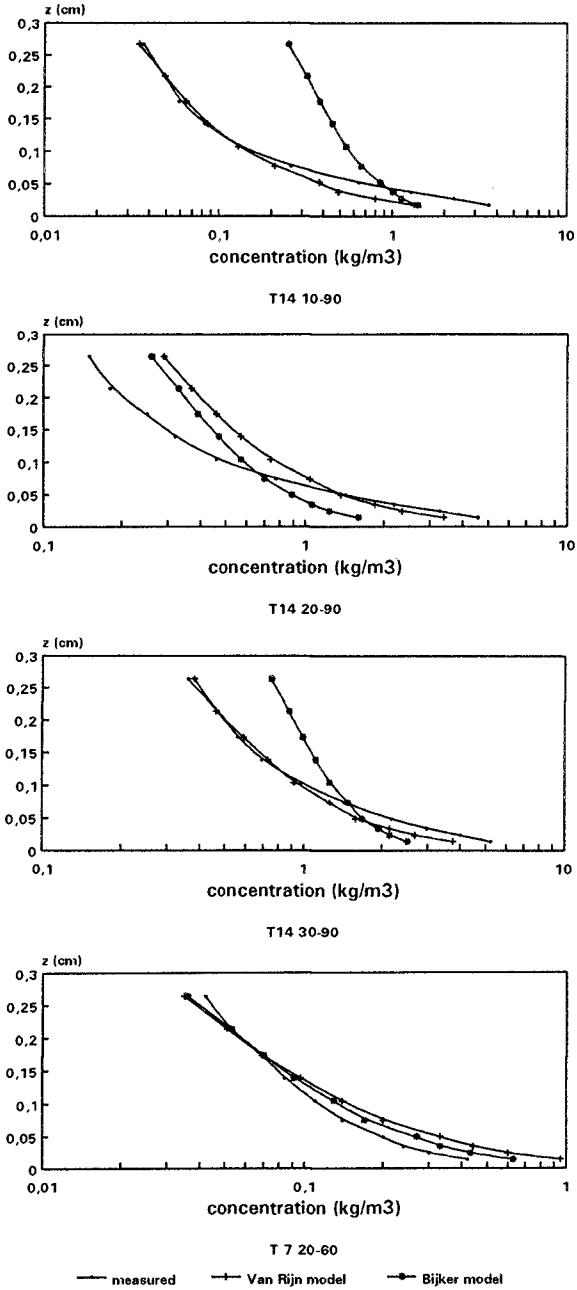


Figure 4 Measured and computed concentration profiles

#### 4. Field experiments

##### 4.1 Site description

The field experiments were performed at the central part of the Dutch coast near Egmond aan Zee. The hydrodynamics near Egmond aan Zee are characteristic for a mixed-energy coast of a semi-enclosed sea. The incoming waves from the North Sea have a mean annual wave height of 1.3 m and come from southwestern to northern directions. The mean semi-diurnal tidal range is 1.65 m, with a maximum range at spring tide of 2.10 m and a minimum range at neap tide of 1.40 m. The tidal curve near Egmond is asymmetrical with a flood period of 4 hours and an ebb period of 8 hours. The morphology of the beach and nearshore zone in this area is characterized by an outer and an inner nearshore bar in the subtidal zone and a swash bar on the beach.

The sediments in the area are well sorted and composed of fine to medium sand. The mean grain size ranges between 250 and 350  $\mu\text{m}$ . Most of the sediments of the bed surface contain shells (especially in the troughs between the bars) or shell fragments (especially in the swash zone, close to the toe of the beach face).

##### 4.2 Measurements

Detailed measurements of the sediment transport processes in the inner nearshore zone were executed with the use of a small platform. The platform is a scaffold construction of 2.5 meter in length and width at 2.5 meter above the bed. During a measurement day the platform is positioned on a location within the inner nearshore zone. The platform is pulled through the water with a tractor and a winch standing on the beach. The platform is equipped with a capacitance wire, three electromagnetic flow devices, two optical backscatterance devices and a pump sampling system. All these instruments are installed on the seaward exposed site of the platform.

The capacitance wire (CAP) measures the free surface elevations of the water column. The three electromagnetic flow devices (EMF) measure the longshore and cross-shore velocity components in the horizontal plane at three heights above the bed.

The cross-shore micro-morphology of the bed over about 2.5 m was determined by use of a mechanical feeler system consisting of a small trolley connected to a rod movable along one side of the platform. The recorded series of the bed morphology have a spatial resolution of 0.05 m.

Herein, the time-averaged sediment concentration profiles and transport rates are discussed.

##### 4.3 Time-averaged concentrations

Time-averaged concentration profiles at different relative wave heights ( $H_s/h$ ) are shown in Figure 5 and 6.

Figure 5 shows measured concentration profiles under various wave conditions in the surf zone with water depths ranging from 0.7 to 1.2 m. The relative wave heights ( $H_s/h$ ) were in the range of 0.4 to 0.7. The near-bed concentrations are in the range of 0.2 to 2 gr/l. The near surface concentrations are in the range of 0.01 to 0.5 gr/l. A clear influence of the relative wave height can be observed. The near-bed concentrations increase for an increasing relative wave height. The concentration profiles also become more uniform for increasing relative wave height.

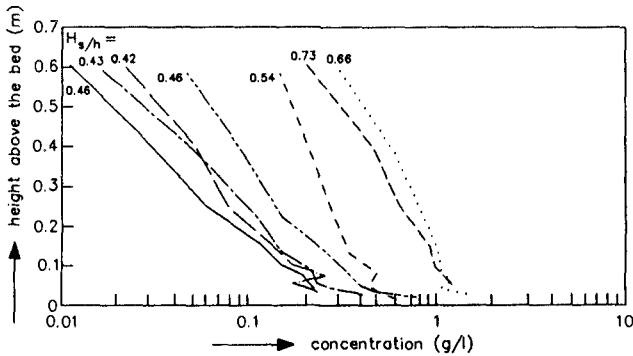


Figure 5 Sand concentration profiles in surf zone

Figure 6 shows concentration profiles in the swash zone with strongly plunging breaking waves. The measured concentrations are a factor 10 larger with near-bed concentrations in the range of 10 to 20 gr/l and a large mixing effect over the depth (more uniform profiles) can be observed.

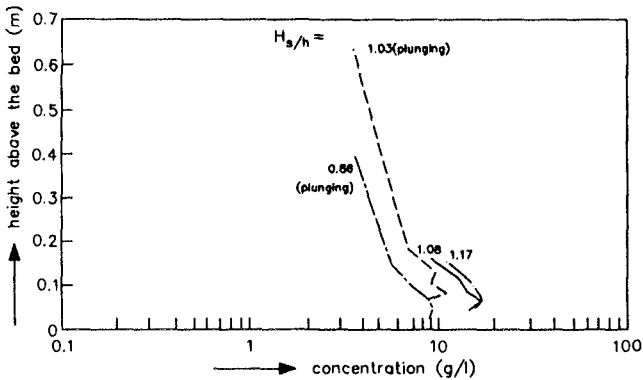


Figure 6 Sand concentration profiles in swash zone

Figure 7 shows the ratio of the concentrations measured at  $z = 0.01$  m and at  $z = 0.1$  m above the bed as a function of relative wave height ( $H_s/h$ ). The ratio sharply decreases for  $H_s/h$  larger than 0.2. A constant value of 2 can be observed for  $H_s/h$  larger than 0.6 which means almost uniform concentration profiles due to the breaking process.

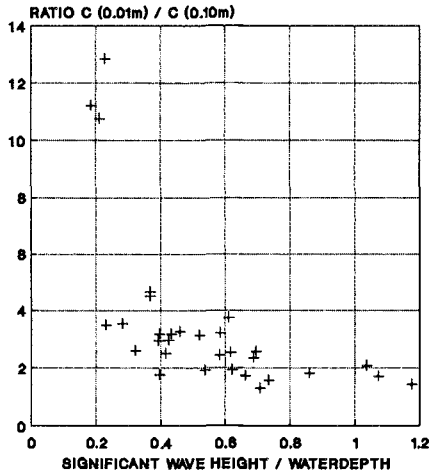


Figure 7 Ratio of concentration at  $z = 0.01$  m and at  $z = 0.1$  m above the bed

Figure 8 shows measured concentrations at  $z = 0.01$  m above the bed as a function of the peak orbital velocity near the bed under the wave crest. Although the scatter is relatively large, the concentrations show an increasing trend for increasing orbital velocities. The experimental results of Ribberink and Al Salem (1991, 1992) measured in wave tunnel conditions are also shown. The relatively large values at low orbital velocities are related to the presence of ripples which are gradually washed out for increasing orbital velocities ( $\hat{U} = 0.8$  m/s).

Equation (4) was used to compute the concentrations at  $z = 0.01$  m above the bed. Reasonable agreement with measured values can be observed. A similar function proposed by Bijker (1971,1978) was also used (b-factor = 1). As can be observed the Bijker-formula yields almost constant concentrations.

Measured and computed concentration profiles for a range of conditions are shown in Figures 9 and 10. The wave-related bed roughness was taken  $k_{s,w} = 0.05$  m for ripples and  $k_s = 0.01$  m for sheet flow conditions. The significant wave height and the peak period were taken as the characteristic wave parameters. The  $\delta_s$ -parameter expressing the thickness of the near-bed sediment mixing layer in the surfzone, which is an unknown parameter, was used as a calibration parameter. A value of  $\delta_s = 0.2$  m gave good results for all conditions. The ratio of  $\delta_s/h$  shows an increasing trend for increasing values of  $H_s/h$ , see Fig. 11.

Analysis of measured and computed concentration profiles shows reasonably good results for  $H_s/h$ -values upto 0.75 (surf zone), see Figs. 9 and 10. For  $H_s/h$ -values larger than 0.75 (plunging waves in the swash zone) the computed concentrations are systematically smaller than the measured concentrations. Increase of the wave-related bed roughness from  $k_{s,w} = 0.01$  m to  $k_{s,w} = 0.04$  m yields larger concentrations, but the computed values are still a factor of 2 too small. Furthermore, a bed roughness of  $k_{s,w} = 0.04$  m in the swash zone is not realistic. Based on this, it is concluded that the time-averaged concentrations in the swash zone cannot be computed using an equilibrium model concept. The hydrodynamic processes in the swash zone with a relatively steep upsloping bed are strongly non-uniform. Vertical as well as horizontal convective processes are important and should be modeled properly.

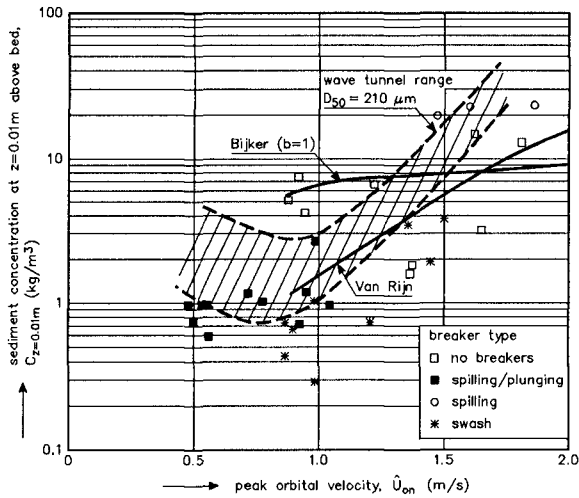


Figure 8 Concentration at  $z = 0.01$  m above the bed

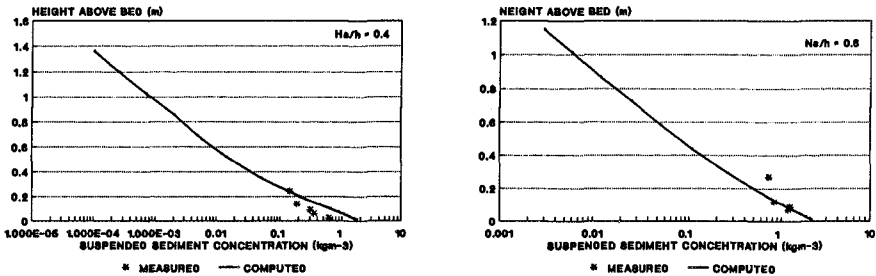


Figure 9 Measured and computed concentration profiles

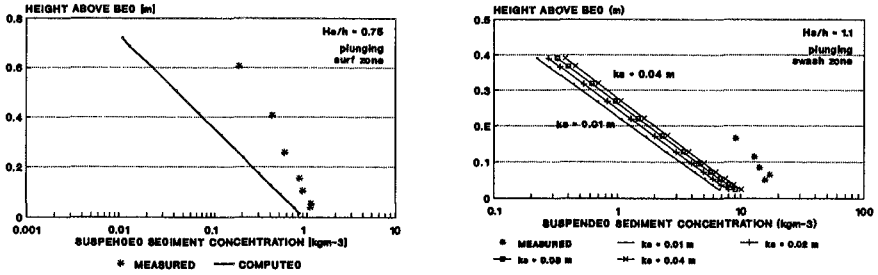


Figure 10 Measured and computed concentration profiles

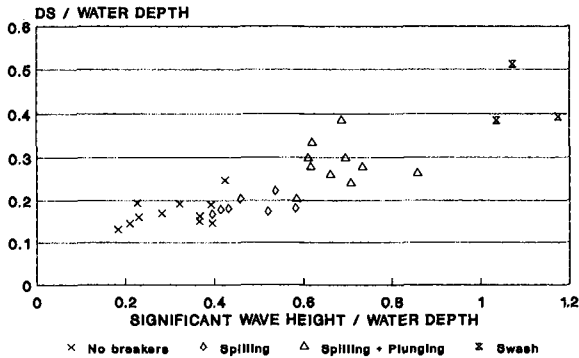


Figure 11 Near-bed sediment mixing layer ( $\delta_s/h$ )

5. Conclusions

The following conclusions are given:

- the current velocity hardly affects the near-bed sediment concentrations; the wave motion is dominant
- the sediment concentrations are maximum when the waves are directed normal to the current (in the ripple regime)
- the sediment concentrations show a large increase under plunging breaking waves, especially in the swash zone
- the concentrations in the swash zone are not locally determined (space lag)
- computed concentration profiles show reasonable agreement with measured values for relative wave heights upto  $H_s/h = 0.7$ .

REFERENCES

Bosman, J.J., Van der Velden, E. and Hulsbergen, C.H., 1987. Sediment Concentration Measurements by Transverse Suction. Coastal Engineering, No. 12.  
 Bijker, E.W., 1971. Longshore Transport Computations. Journal of Waterways, Harbour and Coastal Engineering, Vol. 97, WW4.

- Bijker, E.W., 1978. Lecture Notes Coastal Engineering. Dep. Coastal Engineering, Delft Univ. of Technology, Delft, The Netherlands.
- Kroon, A. and Van Rijn, L.C., 1992. Suspended Sediment Fluxes in the Nearshore Zone at Egmond aan Zee, The Netherlands. Dep. Phys. Geography, Univ. of Utrecht, The Netherlands.
- Ribberink, J.S. and Al Salem, A., 1991. Sediment Transport, Concentrations and Bed Forms in Simulated Asymmetric Wave Conditions. Report H840, Part IV, Delft Hydraulics, Delft, The Netherlands.
- Ribberink, J.S. and Al Salem, A., 1992. Sediment Transport, Concentrations and Bed Forms in Simulated Asymmetric Wave Conditions Report H840, Part V, Delft Hydraulics, Delft, The Netherlands.
- Van Rijn, L.C., 1989. Handbook of Sediment Transport by Current and Waves. Delft Hydraulics, Delft, The Netherlands.
- Van Rijn, L.C., 1990. Principles of Fluid Flow and Surface Waves in Rivers, Estuaries, Seas and Oceans. Aqua Publications, P.O. Box 9896, Amsterdam, The Netherlands.
- Van Rijn, L.C., 1991. Data Base, Sediment Concentration Profiles and Transport for Currents and Waves. Delft Hydraulics, Delft, The Netherlands.
- Van Rijn, L.C., 1993. Principles of Sediment Transport in Rivers, Estuaries, Coastal Seas and Oceans (in Press). Aqua Publications, P.O. Box 9896, Amsterdam, The Netherlands.
- Van Rijn, L.C. et al, 1993. Transport of Fine Sands by Currents and Waves. Journal of Waterways, Port, Coastal and Ocean Engineering, ASCE, March (in Press).